An *Ab Initio* Molecular Orbital Study on the Amino Alcohol-Promoted Reaction of Dialkylzincs and Aldehydes

Masashi Yamakawa[†] **and Ryoji Noyori***[,‡]

Contribution from Kinjo Gakuin University, Omori, Moriyama, Nagoya 463, Japan, and the ERATO Molecular Catalysis Project, Research Development Corporation of Japan, 1247 Yachigusa, Yakusa-cho, Toyota 470-03, Japan

Received February 20, 1995[⊗]

Abstract: The β-dialkylamino alcohol-promoted reaction of dialkylzincs and aldehydes has been studied by *ab initio* molecular orbital calculations using a model system consisting of 2-aminoethanol, dimethylzinc, and formaldehyde. In the organometallic addition reaction, methylzinc alkoxide **1** formed from dimethylzinc and 2-aminoethanol by elimination of methane acts as an actual catalyst, which exists in equilibration with stereoisomeric dimers **2**. Sterically less congested *anti*-**2** is more stable than *syn*-**2** by 3.1 kcal/mol. The tricoordinate Zn compound **1**, acting as a bifunctional catalyst, assembles dimethylzinc and formaldehyde via **3** or **4** to form the product-forming complex **5**. The frontier MOs and structure of **5** indicate that the formation of the mixed-ligand Zn complexes considerably increases the nucleophilic character of the $Zn-CH_3$ group and electrophilic property of the aldehyde. As a consequence, **5** undergoes intramolecular alkyl migration to produce zinc ethoxide **6** which has a bridged structure. This turnover-limiting reaction occurs via the 4/4-bicyclic transition structure, *anti*- or *syn*-**10**, where the methyl group migrates with retention of configuration. The six-membered cyclic transition state that causes the alkyl migration with inversion of configuration is of higher energy. The final product **6** which is viewed as a complex of **1** and Zn alkoxide **7**, upon interaction with dimethylzinc or formaldehyde, collapses into **3** or **4**, respectively, and **9** (a tetramer of **7**). The structural characteristics of the intermediates, products, and transition states are described. This calculation also clarifies the origin of the ligand acceleration; why the reaction is effected only when a few mol %, but not 0% or 100%, of an amino alcohol is employed. The high stability of the final tetrameric Zn alkoxide **9** prevents the undesired product inhibition of the catalytic reaction. The relative stability of the catalyst dimers, *syn*- and *anti*-**2**, is consistent with the chiral amplification phenomena experimentally observed with (2*S*)-3-*exo*-(dimethylamino)-borneol. The presence of the amino moiety plays a significant role in the dissociation of the dimers.

Dialkylzincs are inert to aldehydes in hydrocarbon solvents at ambient temperatures. However, a β-dialkylamino alcohol facilitates the addition reaction to a great extent, giving after an aqueous workup the corresponding secondary alcohols.[1] Figure 1 illustrates an enantioselective version of the reaction using (2*S*)-3-*exo*-(dimethylamino)isoborneol (DAIB) as a chiral source.[1,2] Here the stoichiometry of the dialkylzinc and amino alcohol appears to markedly affect reactivity. *When 100 mol % of the amino alcohol is added to dialkylzinc, no alkylation takes place; instead, addition of a small amount of the amino alcohol affords in high yield the alkylation product.* Actually, the reaction of the dialkylzinc and aldehyde is catalyzed by an alkylzinc alkoxide that is formed from the dialkylzinc and DAIB by elimination of an alkane. Interestingly, the ethylation reaction with DAIB in 15% ee gives the alkylation product in 95% ee, which is close to the 98% ee obtained with enantiomerically pure DAIB.[3] This article describes an *ab initio* molecular orbital (MO) study on the mechanism of this interesting reaction using a model system. The purpose of this study is to elucidate the structures, stabilities, and reactivities of the organozinc complexes and the reaction course. The detailed calculations not only shed light on the properties of experimentally inaccessible short-lived intermediates and transition structures but also dictate some modifications to the original postulates on the reaction mechanism.[1,4] In addition, this study explains the origins of the catalytic efficiency and chirality

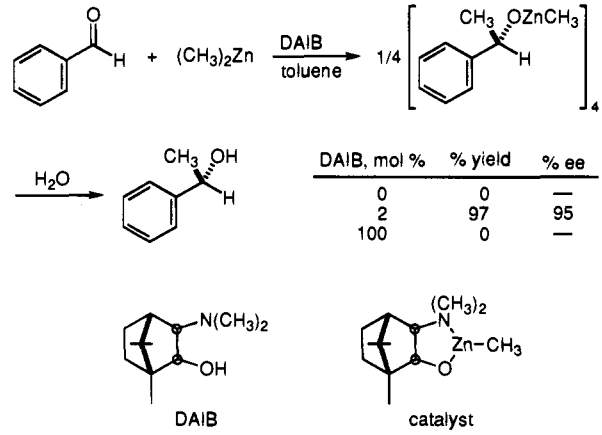

Figure 1. Enantioselective reaction of dimethylzinc and benzaldehyde promoted by DAIB.

[†] Kinjo Gakuin University.

[‡] Research Development Corporation of Japan. Permanent address: Department of Chemistry, Nagoya University, Chikusa, Nagoya 464-01, Japan.

[⊗] Abstract published in *Advance ACS Abstracts*, June 1, 1995.

(1) Reviews: (a) Noyori, R. *Asymmetric Catalysis in Organic Synthesis*; John Wiley & Sons: New York, 1994; Chapter 5. (b) Noyori, R.; Kitamura, M. *Angew. Chem., Int. Ed. Engl.* **1991**, *30*, 49–69. (c) Soai, K.; Niwa, S. *Chem. Rev.* **1992**, *92*, 833–856.

(2) Kitamura, M.; Suga, S.; Kawai, K.; Noyori, R. *J. Am. Chem. Soc.* **1986**, *108*, 6071–6072. Noyori, R.; Suga, S.; Kawai, K.; Okada, S.; Kitamura, M.; Oguni, N.; Hayashi, M.; Kaneko, T.; Matsuda, Y. *J. Organomet. Chem.* **1990**, *382*, 19–37.

(3) (a) Noyori, R.; Suga, S.; Kawai, K.; Okada, S.; Kitamura, M. *Pure Appl. Chem.* **1988**, *60*, 1597–1606. (b) Kitamura, M.; Okada, S.; Suga, S.; Noyori, R. *J. Am. Chem. Soc.* **1989**, *111*, 4028–4036. (c) Kitamura, M.; Suga, S.; Niwa, M.; Noyori, R. *J. Am. Chem. Soc.* **1995**, *117*, 4832–4842. See also: Oguni, N.; Matsuda, Y.; Kaneko, T. *J. Am. Chem. Soc.* **1988**, *110*, 7877–7878.

0002-7863/95/1517-6327$09.00/0

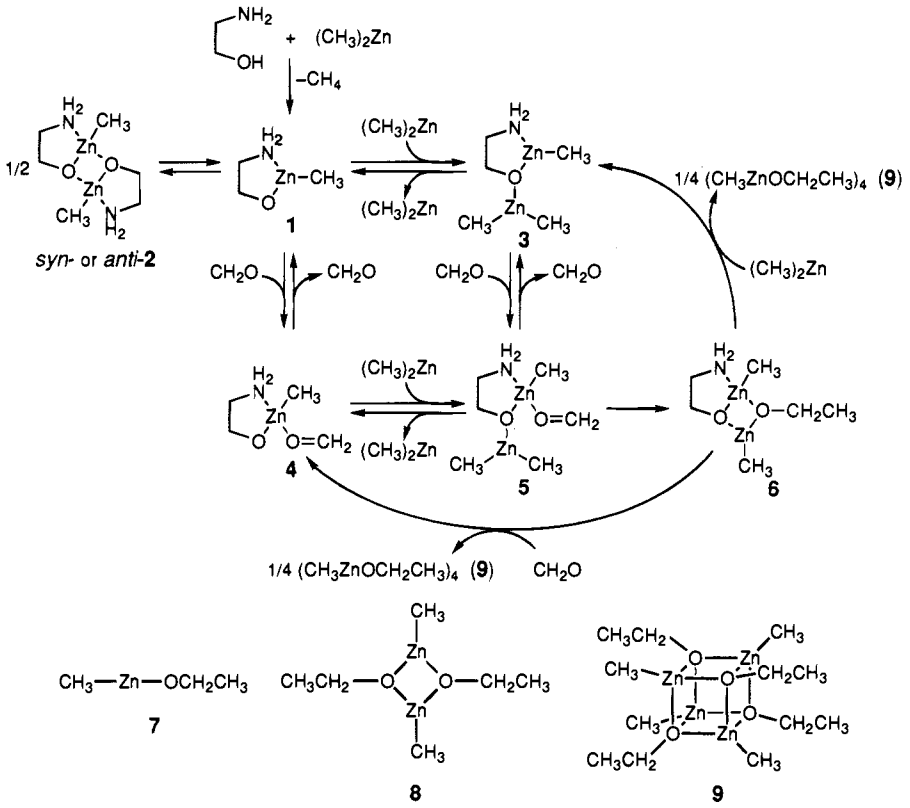

Figure 2. The catalytic cycle of the amino alcohol-promoted reaction of dimethylzinc and formaldehyde.

amplification as well as the necessity to use amino alcohols instead of simple alkanols as promoters.

Results and Discussion

We selected a model reaction of dimethylzinc and formaldehyde promoted by 2-aminoethanol. For each organometallic structure a full optimization was performed at the restricted Hartree–Fock (RHF) level using energy gradient techniques with an all electron [8s4p2d]/(14s9p5d) basis set[5] for Zn and 3-21G for C, H, N, and O. The energy determination was made using a single point restricted second-order Møller–Plesset (RMP2) perturbation calculation with frozen core approximation on the RHF local minimum and/or transition geometry. The calculations employed the same basis function as in the RHF calculation for Zn and 6-31G* for other atoms. The drawing of the frontier MOs as well as Mulliken population analysis was performed on the basis of the RHF calculations. All of the MO calculations on the organozinc compounds were carried out with the GAUSSIAN 92 program.[6]

Summary. The calculations are in accord with the operation of the mechanism of Figure 2 for the overall catalytic alkylation. The reaction of 2-aminoethanol and dimethylzinc first generates the methylzinc alkoxide **1** acting as catalyst, which is in equilibrium with the dimer **2**. The tricoordinate Zn complex **1** acts as both Lewis acid and base at the Zn and oxygen center, respectively. Thus, **1** reacts with dimethylzinc to give the dinuclear Zn compound **3**, which then assembles formaldehyde to form the product-forming, mixed-ligand complex **5**. The same compound is also derived from **1** by initial coordination of formaldehyde followed by its combination with dimethylzinc: **1** → **4** → **5**. The reversible formation of **5** is followed by the intramolecular alkyl-transfer reaction leading to **6**. In the presence of dimethylzinc or formaldehyde, **6** collapses to methylzinc ethoxide **7** and the intermediate **3** or **4**, respectively, completing the catalytic cycle. The alkylation product **7** is further stabilized by forming the cyclic dimer **8** and finally, the cage tetramer **9**. This model system is very close to the real reaction of Figure 1, the differences being the lack of the chiral skeleton and alkyl groups at the nitrogen of the amino alcohol as well as the phenyl substituent in the aldehyde substrate. In the actual reaction, the process corresponding to **5** → **6** is the turnover-limiting and stereodetermining step.[1a,b,3b]

Organozinc Intermediates and Products. Table 1 lists calculated energies of the compounds involved in the catalytic reaction in Figure 2. The calculated three-dimensional structures of the starting materials and organozinc intermediates and products, **1**–**9**, are given in Figure 3.

The methylzinc aminoalkoxide **1** has a planar structure at Zn. However, the Zn atom is not fully sp^2-hybridized, since the coordination of the amino function to Zn is rather weak.[7] The tricoordinate Zn atom has a bent structure possessing an O(2)–Zn(1)–C(6) angle of 158.9°, which is closer to a sp-like structure (180°) rather than a regular sp^2 structure (120°). In fact, the N(5)–Zn(1) dative bond is longer than those observed for Zn–N covalent bonds.[8] As envisaged from the frontier MOs of **1** given in Figure 4, the LUMO develops heavily on the Zn atom and the HOMO on the neighboring oxygen atom. The lone pair electrons of the oxygen cannot be used for the π interaction with Zn, since the tricoordinate Zn(II) atom has an

(4) (a) Itsuno, S.; Fréchet, J. M. J. *J. Org. Chem.* **1987**, *52*, 4140–4142. (b) Evans, D. A. *Science* **1988**, *240*, 420–426. (c) Corey, E. J.; Hannon, F. J. *Tetrahedron Lett.* **1987**, *28*, 5233–5236. Corey, E. J.; Hannon, F. J. *Tetrahedron Lett.* **1987**, *28*, 5237–5240. (d) Corey, E. J.; Yuen, P.-W.; Hannon, F. J.; Wierda, D. A. *J. Org. Chem.* **1990**, *55*, 784–786.

(5) Poirier, R.; Kari, R.; Csizmadia, I. G. *Handbook of Gaussian Basis Sets*; Elsevier: Amsterdam, 1985.

(6) Frisch, M. J.; Trucks, G. W.; Head-Gordon, M.; Gill, P. M. W.; Wong, M. B.; Foresman, J. B.; Johnson, B. G.; Schlegel, H. B.; Robb, M. A.; Replogle, E. S.; Gomprets, R.; Andres, J. S.; Raghavachari, K.; Binkley, J. S.; Gonzalez, C.; Martin, R. L.; Fox, D. J.; Defrees, D. J.; Baker, J.; Stewart, J. J. P.; Pople, J. A. *Gaussian-92*; Gaussian Inc.: Pittsburgh, PA, 1992.

(7) Haaland, A. *Angew. Chem., Int. Ed. Engl.* **1989**, *28*, 992–1007.

(8) For example: Haaland, A.; Hedberg, K.; Power, P. P. *Inorg. Chem.* **1984**, *23*, 1972–1975.

Table 1. Calculated Energies (Hartree) for Dimethylzinc, Formaldehyde, 2-Aminoethanol, and Organozinc Compounds and Imaginary Frequencies (cm^{-1}) for Transition States (TS)

compound	HF//HF	MP2//HF	imaginary frequency
dimethylzinc	−1856.4189	−1857.3371	
formaldehyde	−113.2218	−114.1668	
2-aminoethanol	−207.9406	−209.7014	
1	−2024.4223	−2026.7557	
anti-**2**	−4048.9271	−4053.5765	
syn-**2**	−4048.9227	−4053.5716	
3	−3880.8741	−3884.1182	
4	−2137.6705	−2140.9407	
5	−3394.1189	−3998.3019	
μ-**5**	−3994.1095	−3998.2921	
6	−3994.1953	−3998.3780	
7	−1969.6836	−1971.5515	
8	−3939.4653	−3943.1806	
9	−7879.0174	−7886.4514	
anti-**10** (TS)	−3994.0945	−3998.2822	343i
syn-**10** (TS)	−3994.0933	−3998.2775	308i
11 (TS)	−3994.0827	−3998.2713	659i
13	−1969.6499	−1971.5109	
14	−1969.5980	−1971.4643	468i
15	−2137.6885	−2140.9696	
16 (TS)	−2137.6111	−2140.8894	461i

s type vacant orbital. The absence of the O to Zn electron donation provides **1** with its eminent bifunctional catalytic property.

The tricoordinate complex **1** which contains a Lewis acidic Zn and a basic oxygen center undergoes electrocomplementary dimerization[9] to form a chiral or achiral compound, *syn*- or *anti*-**2**, respectively. The formation of *syn*-**2** occurs with an exothermicity of 37.8 kcal/mol, or 18.9 kcal/mol **1**. The syn stereoisomer with C_2 symmetry has a puckered Zn_2O_2 four-membered ring, where the O(2)−Zn(1)−O(8) angle, 80.0°, is much smaller than the Zn(1)−O(2)−Zn(7) angle, 98.0°. Thus, the Zn atoms have an sp^3 configuration, while the oxygen atoms have a substantially sp^2 character. The lengths of the two kinds of Zn−O bonds are similar because of the comparable covalent and dative bonding contributions.[7] In going from monomer **1** to the syn dimer, the Zn−O bond is elongated by 9%. The sp^3 hybridization of the Zn atom elongates the Zn−CH_3 bonds. The stereoisomer *anti*-**2** is a C_i symmetrical compound with a planar Zn_2O_2 four-membered ring in contrast to the puckered structure of *syn*-**2**. The structural change caused by the dimerization is similar to that in the syn dimerization. The formation of *anti*-**2** is exothermic by 40.9 kcal/mol, or 20.5 kcal/mol **1**, and this dimer is more stable than the syn isomer by 3.1 kcal/mol. The relative stabilities are readily understood by considering the difference in the extent of the steric congestion of the syn- and anti-5/4/5 tricyclic skeletons.

The basic oxygen atom in **1** interacts with dimethylzinc to form the dinuclear Zn complex **3** with an exothermicity of 16.0 kcal/mol. The Lewis base coordination to dimethylzinc results in a 2% increase of the Zn(7)−CH_3 bond lengths and a decrease in the CH_3−Zn−CH_3 angle from 180°[10] to 152.4°.

Since **1** has a Lewis acidic Zn center, it accepts formaldehyde via an oxygen nonbonding orbital[11,12] to give the tetrahedral Zn complex **4** with exothermicity of 11.4 kcal/mol. Although the structure of **1** is modified to some extent by such interaction, the Zn geometry is only slightly pyramidized (sum of these bond angle, 353.8°). The distance of 2.119 Å between O(2) and a hydrogen atom of C(11) suggests the presence of a bonding interaction (cf. sum of the van der Waals radii, 2.72 Å). The C=O bond is 1% elongated from the free state.

The bifunctional complex **1** accommodates both dimethylzinc and formaldehyde. The key product-forming complex **5** is generated either by the reaction of **3** and formaldehyde (ΔE = −10.6 kcal/mol) or by the complexation of **4** and dimethylzinc (ΔE = −15.1 kcal/mol). This complex is 26.6 kcal/mol more stable than a standard 1:1:1 mixture of catalyst **1**, dimethylzinc, and formaldehyde. In the dinuclear mixed-ligand complex, the tetracoordinate Zn(1) atom has a pyramidal geometry, and the tricoordinate Zn(7) atom has a flat, sp-to-sp^2 geometry with a CH_3−Zn(7)−CH_3 angle of 148.2°. The tricoordinate O(2) atom is planar, as is seen in **3**. In comparison to the structure of catalyst **1**, the Zn(1)−O(2) bond is 3% longer, and the Zn(1)−N(5) bond becomes 2% shorter. The formaldehyde uses an oxygen nonbonding orbital for the coordination to Zn(1). The carbonyl double bond is 0.7% longer than that of free formaldehyde, and the methylene carbon is endowed with an electrophilic character.[11,12] The most notable feature is the long Zn(7)−CH_3 distances, which is 2−3% longer than the value in free dimethylzinc, suggesting the great increase of the nucleophilic character of the methyl groups. The Zn(1)−CH_3 bond is much shorter. The Zn(1)−N(5) bond is anti-coplanar with the formaldehyde plane with respect to the Zn(1)−O(10) bond, as judged from the N(5)−Zn(1)−O(10)−C(11) dihedral angle of 179.2°. Although the conformation of the formaldehyde is highly flexible, its syn stereoisomer is not a local minimum.

The calculation predicts the presence of an entirely different local minimum, μ-**5**, containing a bridging formaldehyde.[13] This structure, which is less stable than **5** by 6.2 kcal/mol, is characterized by the presence of the weak interaction between Zn(7) and aldehyde O(10). The C(11)=O(10) length is identical with that of **5**. The O(10) atom is bridging over Zn(1) and Zn(7) using its two nonbonding orbitals, but because of the difference in Lewis acidity of the two Zn atoms, the strengths of the two interactions are not equal; Zn(1)−O(10), 2.249 Å, is shorter than Zn(7)−O(10), 2.679 Å. The latter is weak

(9) (a) van der Schaaf, P. A.; Wissing, E.; Boersma, J.; Smeets, W. J. J.; Spek, A. L.; van Koten, G. *Organometallics* **1993**, *12*, 3624−3629. (b) van Vliet, M. R. P.; van Koten, G.; Buysingh, P.; Jastrzebski, J. T. B. H.; Spek, A. L. *Organometallics* **1987**, *6*, 537−546. (c) Jastrzebski, J. T. B. H.; Boersma, J.; van Koten, G.; Smeets, W. J. J.; Spek, A. L. *Recl. Trav. Chim. Pays-Bas* **1988**, *107*, 263−266. (d) van der Steen, F. H.; Boersma, J.; Spek, A. L.; van Koten, G. *Organometallics* **1991**, *10*, 2467−2480. (e) Bolm, C.; Schlingloff, G.; Harms, K. *Chem. Ber.* **1992**, *125*, 1191−1203. (f) Olmstead, M. M.; Power, P. P.; Shoner, S. C. *J. Am. Chem. Soc.* **1991**, *113*, 3379−3385.

(10) Almenningen, A.; Helgaker, T. U.; Haaland, A.; Samdal, S. *Acta Chem. Scand., Part A* **1982**, *36*, 159−166.

(11) Reetz, M. T.; Hüllmann, M.; Massa, W.; Berger, S.; Rademacher, P.; Heymanns, P. *J. Am. Chem. Soc.* **1986**, *108*, 2405−2408. Power, M. B.; Bott, S. G.; Atwood, J. L.; Barron, A. R. *J. Am. Chem. Soc.* **1990**, *112*, 3446−3451. Shambayati, S.; Crowe, W. E.; Schreiber, S. L. *Angew. Chem., Int. Ed. Engl.* **1990**, *29*, 256−272. Shambayati, S.; Schreiber, S. L. In *Comprehensive Organic Synthesis*; Trost, B. M., Fleming, I., Eds.; Pergamon Press: Oxford, 1991; Vol. 1, Chapter 1.10. Faller, J. W.; Ma, Y. *J. Am. Chem. Soc.* **1991**, *113*, 1579−1586. Corey, E. J.; Loh, T.-P.; Sarshar, S.; Azimioara, M. *Tetrahedron Lett.* **1992**, *33*, 6945−6948. Denmark, S. E.; Almstead, N. G. *J. Am. Chem. Soc.* **1993**, *115*, 3133−3139. Müller, B.; Ruf, M.; Vahrenkamp, H. *Angew. Chem., Int. Ed. Engl.* **1994**, *33*, 2089−2090.

(12) (a) LePage, T. J.; Wiberg, K. B. *J. Am. Chem. Soc.* **1988**, *110*, 6642−6650. (b) Branchadell, V.; Oliva, A. *J. Am. Chem. Soc.* **1991**, *113*, 4132−4136; Dalton, D. M.; Fernández, J. M.; Emerson, K.; Larsen, R. D.; Arif, A. M.; Gladysz, J. A. *J. Am. Chem. Soc.* **1990**, *112*, 9198−9212. (c) Gung, B. W.; Wolf, M. A. *J. Org. Chem.* **1992**, *57*, 1370−1375. (d) Goodman, J. M. *Tetrahedron Lett.* **1992**, *33*, 7219−7222. (e) Jonas, V.; Frenking, G.; Reetz, M. T. *J. Am. Chem. Soc.* **1994**, *116*, 8741−8753.

(13) Palm, J. H.; MacGillavry, C. H. *Acta Crystallogr.* **1963**, *16*, 963−968. Verbist, J.; Meulemans, R.; Piret, P.; Van Meerssche, M. *Bull. Soc. Chim. Belg.* **1970**, *79*, 391−395. Rao, C. P.; Rao, A. M.; Rao, C. N. R. *Inorg. Chem.* **1984**, *23*, 2080−2085. Beauchamp, A. L.; Olivier, M. J.; Wuest, J. D.; Zacharie, B. *Organometallics* **1987**, *6*, 153−156. Sharma, V.; Simard, M.; Wuest, J. D. *J. Am. Chem. Soc.* **1992**, *114*, 7931−7933. Seebach, D.; Müller, H.-M.; Bürger, H. M.; Plattner, D. A. *Angew. Chem., Int. Ed. Engl.* **1992**, *31*, 434−435.

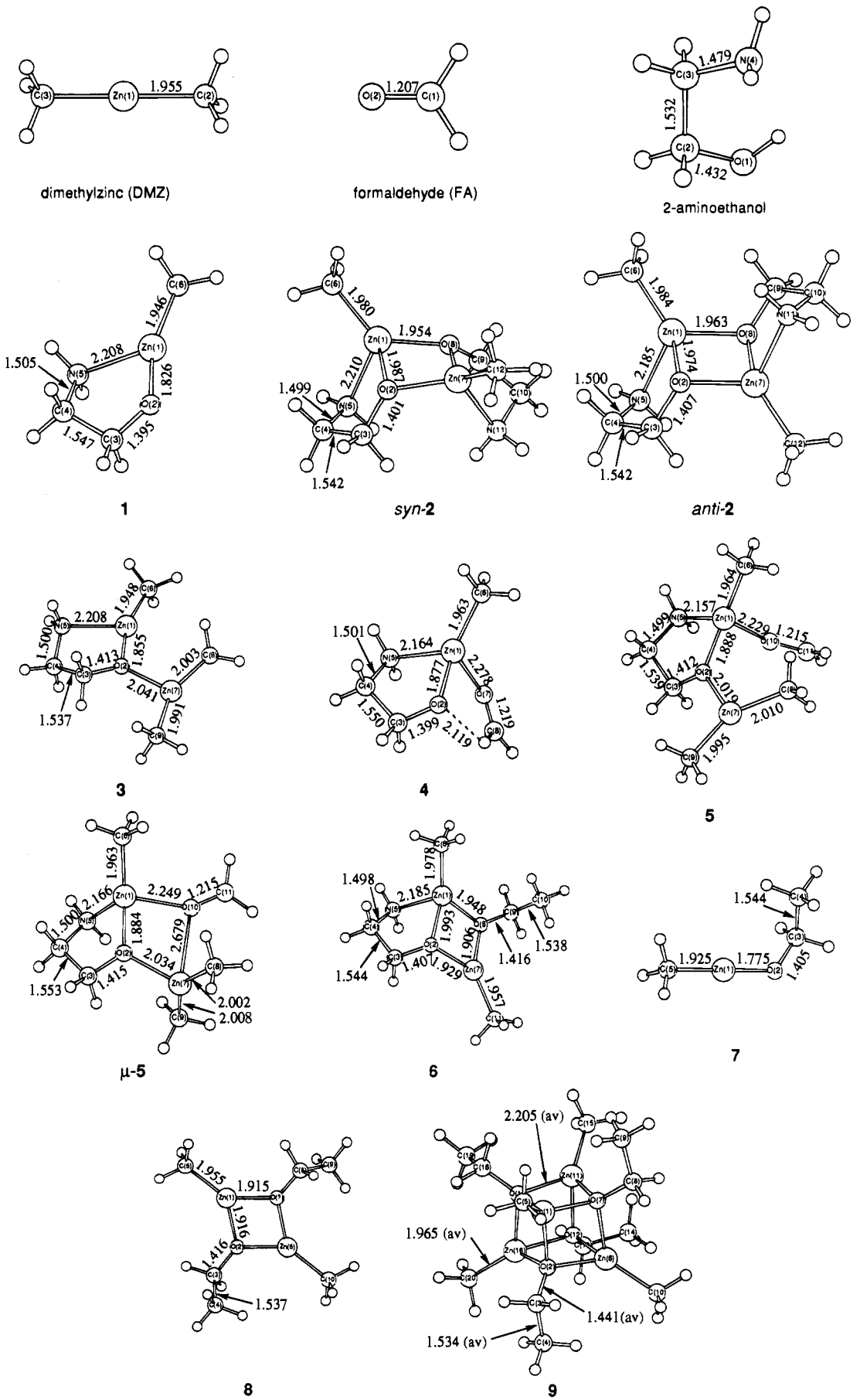

Figure 3. Three-dimensional structures of dimethylzinc, formaldehyde, 2-aminoethanol, and the organozinc complexes **1**–**9**.

coordination determines the conformation of the dimethylzinc moiety. Like in **5**, the C(11)=O(10) bond is 0.7% longer than the free species. Zn(7)–CH_3 distances are also 2–3% longer than in free dimethylzinc.

The alkyl-transfer product **6** is very stable. Its formation from **5** is 47.7 kcal/mol exothermic. This product has a 5/4-fused bicyclic structure with a tetrahedral Zn(1) and a trigonal, planar Zn(7) atom. The Zn_2O_2 four-membered ring is planar. The angular O(2) atom now has a trigonal pyramidal structure with 339.9° for the sum of the three bond angles, but the other bridging oxygen, O(8), is almost planar (sum of three bond angles, 357.9°). Most notably, the Zn(1)−O(2), is even 9% longer than that of **1**. The Zn_2O_2 four-membered ring contains four different Zn−O bonds, whose lengths reflect the nature of hybridization of the elements. Thus, bond length decreases in the order of Zn(1)−O(2) > Zn(1)−O(8) > Zn(7)−O(2) > Zn(7)−O(8). The Zn(1)−O(2) bond is the longest because of the sp^3 configuration of the Zn and O elements, while the Zn(7)−O(8) bond consisting of the sp^2-hybridized atoms is the shortest. The bicyclic complex **6** is a sole local minimum for the product and its open, monocyclic isomer was not found as a local minimum structure.

The dinuclear complex **6** is viewed as an adduct of the catalyst **1** and the alkylation product **7**. The alkylzinc alkoxide **7** has a nearly linear O(2)−Zn(1)−C(5) structure. The product **7** is stabilized by forming the cyclic dimer **8** with the Zn(1)−O(2)−Zn(6) and O(2)−Zn(1)−O(7) angles of 100.0° and 80.0°. The Zn_2O_2 rings of **8** are completely flat, and the four Zn−O bonds have the same length, which is 8% longer than the value in the monomer **7**. The energy of the dimerization is −48.7 kcal/mol, namely, −24.3 kcal/mol of **7**.

The dimeric alkoxide **8** is further stabilized by forming the cubic tetramer **9** (ΔE = −56.6 kcal/mol). This stabilization energy corresponds to 28.3 kcal/mol of **8**. The tetramer **9** has a cage structure where the Zn atoms protrude from a regular octahedral geometry. The alkoxide has an average Zn−O−Zn angle of 97.3° and an O−Zn−O angle of 82.2°. The calculated geometry is in accord with the crystalline structure of methylzinc methoxide tetramer.[14] Each Zn atom in **9** interacts with three oxygen atoms and the Zn−O distances are 14 and 6% longer than those in **7** or **8**, respectively. The Zn−CH_3 bonds are somewhat longer than the bonds in **7** (2%) or **8** (0.6%).

Transition State Structures. The zinc complexes **1**−**5** exist in dynamic equilibrium.[1a,b] As is seen from the structure **5**, upon interaction with catalyst **1**, geometries of formaldehyde and dimethylzinc are modified from the original ones. Such structural changes are well reflected on the frontier MOs of **5** illustrated in Figure 4. The LUMO develops mostly on the aldehyde ligand, while the HOMO is localized on the dimethylzinc moiety. Interestingly, the HOMO develops between the Zn atom and CH_3 groups and also at the rear of the Zn−CH_3 bonds, suggesting the possibility of a methyl migration with both configuration retention and inversion. By forming **5**, the HOMO level of dimethylzinc is raised by 1.31 eV in accord with the increased nucleophilicity, while the LUMO level of formaldehyde is lowered by 1.25 eV enhancing the electrophilicity.

The irreversible reaction, **5** → **6**, is the turnover-limiting step in the catalytic alkylation.[1a,b] Since the energy barriers for rotation about the Zn(1)−O(10) and O(2)−Zn(7) bonds in **5** are rather low (ca. 2 kcal/mol), readily enters the intramolecular alkyl transfer via appropriate geometrical changes. We found three transition structures, *anti*-**10**, *syn*-**10**, and **11**, by the calculations, whose structures are given in Figure 5. Each structure has proved to possess a single imaginary frequency given in Table 1.

The aldehyde and dimethylzinc moieties in **5** are suitably arranged to react with one another by way of *anti*-**10**. The

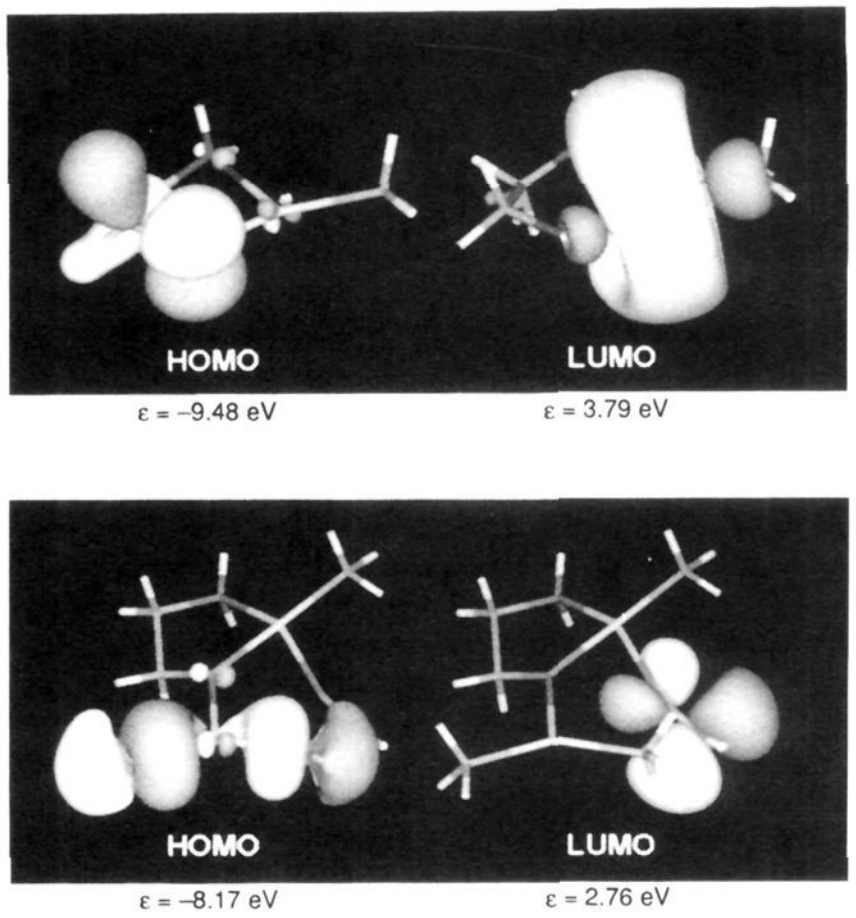

Figure 4. Frontier MOs of the catalyst **1** and product-forming complex **5**. The energy levels of **5** are to be compared with those of CH_2=O (ϵ_{HOMO} = −11.78 eV and ϵ_{LUMO} = 4.01 eV) and $Zn(CH_3)_2$ (ϵ_{HOMO} = −9.48 eV and ϵ_{LUMO} = 3.14 eV).

reaction occurs with an activation energy of 12.4 kcal/mol. The major geometrical changes to maximize the overlap of the MOs occur at O(2) and Zn(7). The simultaneous downward bending of the O(2)−Zn(7) and Zn(7)−C(9) bonds greatly increases the proximity of Zn(7) to O(10). Thus, as Zn(7) of **5** starts to interact with O(10), C(8)H_3 moves to the formaldehyde C(11) atom. The methyl migration takes place with *retention of configuration*. This transition state geometry is characterized by the 4/4-fused bicyclic structure.[4a,b15,16] The interatomic distance between Zn(7) and O(10), 2.534 Å, is much shorter than the sum of the van der Waals radii, 2.91 Å, and clearly indicates the presence of significant attractive interaction. The Zn(7) atom has a planar geometry. The Mulliken population analysis (Table 2) suggests that the interaction between Zn(7) and O(10) is electrostatic in nature and that the covalent contribution is negligible. The charges at the Zn(7) and O(10) atoms are +1.4783 and −0.7939, respectively. Such electrostatic interactions are significant in certain ground-state donor−acceptor complexes such as the $(CH_3)_3N$−$AlCl_3$ adduct.[12e] The population analysis also reveals the high polarity of the Zn(7)−C(8) bond in the transition state. In going from **5** to the transition structure *anti*-**10**, the bond shortening and lengthening take place alternately, O(10)−Zn(1) and O(2)−Zn(7) shorten significantly, but Zn(1)−O(2), Zn(7)−C(8)H_3, and O(10)−C(11) (carbonyl double bond) become substantially longer. The Zn(1)−O(2) distance is 3% elongated in the transition state, and the bond population is reduced by 34%. The Zn(7)−C(8)-H_3 distance is stretched to 2.159 Å (7% increase) from the original length, 2.010 Å, and the distance between the migrating C(8)H_3 and the accepting aldehyde C(11) atom is 2.246 Å. The Zn(7)−C(8)−C(11) angle is 73.8°. It should be noted that Zn(1) keeps a σ-type interaction with formaldehyde throughout the

(14) Shearer, H. M. M.; Spencer, C. B. *Acta Crystallogr., Sect. B: Struct. Sci.* **1980**, *36*, 2046−2050.

(15) Nakamura, M.; Nakamura, E.; Koga, N.; Morokuma, K. *J. Am. Chem. Soc.* **1993**, *115*, 11016−11017.

(16) Jeffery, E. A.; Mole, T. *Aust. J. Chem.* **1970**, *23*, 715−724. See, also: Matteson, D. S. *Organomet. Chem. Rev. A* **1969**, *4*, 263−305. Matteson, D. S. *Organometallics Reaction Mechanisms on the Nontransition Elements*; Academic: New York, 1974; pp 146−147.

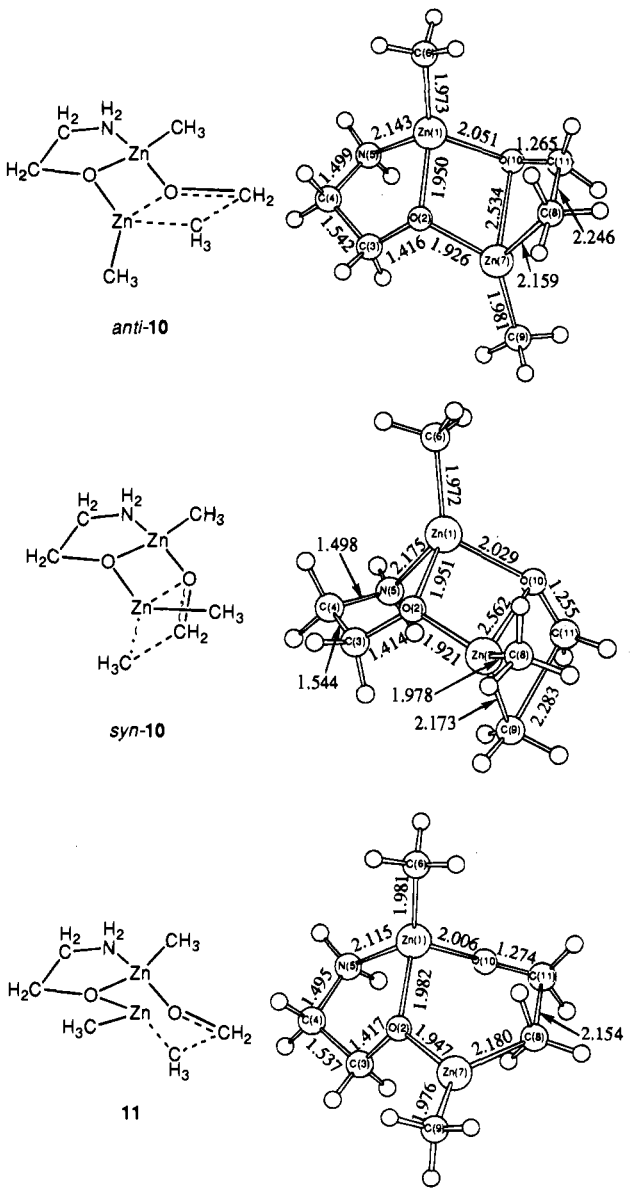

Figure 5. Possible transition structures, **10** and **11**, for the alkyl migration.

reaction and that Zn(7) delivers $C(8)H_3$ to aldehyde C(11) via proper π-face interactions. Thus, the stabilization of the transition structure appears to result from the pericyclic cooperation of the six atoms, Zn(1), O(2), Zn(7), C(8), C(11), and O(10).

The stereoisomeric transition state, *syn*-**10**, was also found. Its structural parameters are very similar to those of the anti isomer and the alkyl migration takes place with retention of configuration. The energy is only 15.3 kcal/mol higher than **5**. Although this structure is less stable than *anti*-**10** by 2.9 kcal/mol, these two possibilities must be seriously considered, when the formaldehyde ligand is replaced by a prochiral aldehyde. The diastereomeric transition structures generate enantioselectivity.[1-3]

We also found a high-energy transition state having a chair-like six-membered structure **11**,[16-18] which is 19.2 kcal/mol higher than **5**. This structure clearly differs from **10** in that the Zn(7) to O(10) interaction is absent and the $C(8)H_3$ group is present approximately in the six-membered plane. The O(2) atom maintains a near-sp^2 geometry (sum of three bond angles, 356.0°). Furthermore the $C(8)H_3$ group now must migrate to the aldehyde carbon with *inversion of configuration*. The shape of the HOMO of **5** (Figure 4) is consistent with this stereochemistry. The bond-forming C(8)–C(11) distnce is 2.154 Å; the breaking Zn(7)–$C(8)H_3$ bond, 2.180 Å, is 8% enlongated from the original length. The Zn(7)–C(8)–C(11) angle, 134.0°, is much larger than those of *anti*- or *syn*-**10**, 73.8° and 73.5°. Furthermore, in comparison to the structure of **5**, O(10)–Zn(1) and O(2)–Zn(7) are shortened, whereas Zn(1)–O(2) and C(11)–O(10) are elongated considerably. Because of the six-membered pericyclic mechanism, the Zn(1)–O(10) distance is shorter and the Zn(1)–O(2) distance is longer than those in *anti*- or *syn*-**10**. Although this geometry resembles that of starting **5**, its involvement in the catalytic reaction is unlikely in view of the high energy. We could not find simple boat-like[19] or flat[15] six-membered transition states.

Table 2. Mulliken Bond Populations and Charges (*e*) for 5, 10, and 11

parameter	5	*anti*-10	*syn*-10	11
Zn(1)–O(2)	0.0662	0.0434	0.0418	0.0401
Zn(1)–N(5)	0.0235	0.0229	0.0177	0.0312
Zn(1)–C(6)	0.1538	0.1589	0.1642	0.1536
Zn(1)–O(10)	0.0140	0.0286	0.0245	0.0303
O(2)–C(3)	0.2724	0.2646	0.2675	0.2711
O(2)–Zn(7)	0.0112	0.0501	0.0489	0.0287
C(3)–C(4)	0.2042	0.2046	0.2099	0.2161
C(4)–C(5)	0.1828	0.1857	0.1903	0.1893
Zn(7)–C(8)	0.1235	0.0087	0.1879	0.0531
Zn(7)–C(9)	0.1552	0.1740	−0.0012	0.1815
Zn(7)–O(10)		0.0101	0.0084	
C(8)–C(11)		0.0479		0.0376
C(9)–C(11)			0.0439	
O(10)–C(11)	0.4458	0.3831	0.4018	0.3939
Zn(1)	+1.4879	+1.4908	+1.5018	+1.5032
O(2)	−1.0082	−1.0097	−1.0120	−0.9981
$C(3)H_2$	+0.3448	+0.3456	+0.3490	+0.3115
$C(4)H_2$	+0.1628	+0.1654	+0.1589	+0.1865
$N(5)H_2$	−0.2354	−0.2218	−0.2249	−0.2252
$C(6)H_3$	−0.7203	−0.7242	−0.7177	−0.7325
Zn(7)	+1.4009	+1.4783	+1.4654	+1.3916
$C(8)H_3$	−0.7490	−0.6172	−0.6816	−0.5459
$C(9)H_3$	−0.7166	−0.7003	−0.6510	−0.6565
O(10)	−0.5938	−0.7939	−0.7940	−0.8274
$C(11)H_2$	+0.6269	+0.5879	+0.6059	+0.5927

Energy Diagram of the Alkylation Reaction. Figure 6 summarizes the energy changes in the reaction, where an equimolar mixture of **1**, dimethylzinc, and formaldehyde is taken as standard. The catalyst **1** is in equilibrium with the stereoisomeric dimers, *syn*- and *anti*-**2**. The reversible formation of the mixed-ligand complex, **5** (stable) or μ-**5** (less stable), is followed by an irreversible methyl migration leading to **6**, where *anti*- and *syn*-**10** are the likely transition states. The overall alkylation giving **6** occurs with high exothermicity, 74.3 kcal/mol. Dissociation of the final product **6** into **1** and methylzinc ethoxide (**7**) is highly endothermic (ΔE = +44.4 kcal/mol), while **7** tends to form the more stable dimer **8** (ΔE = −24.3 kcal/mol **7**) or tetramer **9** (ΔE= −38.5 kcal/mol **7**). On the other hand, the reaction of **6** and formaldehyde, giving **4** and **9**, occurs with an exothermicity of 5.5 kcal/mol. Likewise, the reaction of **6** and dimethylzinc resulting in **3** and **9** is exothermic by 10.0 kcal/mol. The later organozinc displacement is favorable by 4.5 kcal/mol.

Correlation between the Calculations and Experimental Observations. The model reaction system lacks solvent

(17) Soai, K.; Ookawa, A.; Kaba, T.; Ogawa, K. *J. Am. Chem. Soc.* **1987**, *109*, 7111–7115. Niwa, S.; Soai, K. *J. Chem. Soc., Perkin Trans. 1* **1991**, 2717–2720.

(18) Pasynkiewicz, S.; Sliwa, E. *J. Organomet. Chem.* **1965**, *3*, 121–128.

(19) Boat-like six-membered transition states have been proposed in ref 4b–d.

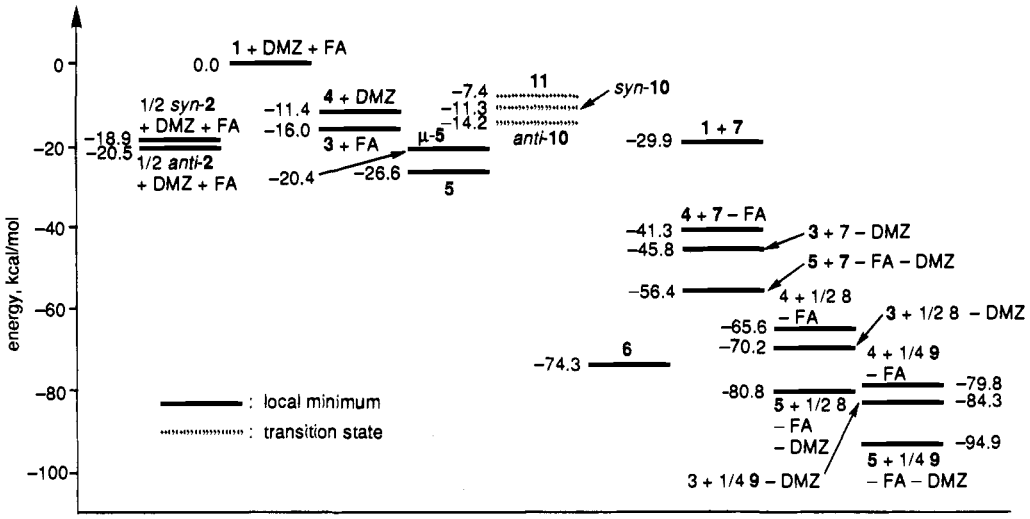

Figure 6. Energy diagram for the reaction of dimethylzinc (DMZ) and formaldehyde (FA) catalyzed by **1**. An equimolar mixture of **1**, DMZ, and FA is taken as standard.

molecules, *N*-alkyl groups and chiral skeletons in the amino alcohol, and carbonyl substituents which play significant roles in determining reactivity and selectivity in the actual catalytic reaction. Nevertheless, the calculated reaction pathway of Figure 2 provides a deep understanding of the DAIB-promoted enantioselective reaction of Figure 1.[1-3]

(a) Structures of Organozinc Compounds. Organozinc species involved in the catalytic cycle are structurally fluxional, undergoing a variety of ligand exchange reactions. Although the previous NMR study failed to elucidate the detailed structures of the short-lived intermediates,[1-3] the present MO calculations on the models provide useful information on the structural characteristics including bonding schemes. In order to explain the facile alkyl scrambling in the reaction, we conceived the presence of alkyl bridges in the dinuclear organozinc complexes.[2,3a,b,20] However, such a possibility can now be excluded from the consideration. The alkyl-bridged species exist only as transient entities or in transition states.

(b) Chirality Amplification. Of particular interest is that the DAIB-promoted alkylation of benzaldehyde (Figure 1) exhibits a significant nonlinear effect between the enantiomeric purities of the DAIB auxiliary and the alcoholic products.[3] Use of only partially resolved DAIB (<20% ee) affords the alkylation products in >90% ee. This unique phenomenon has been interpreted in terms of the relative stabilities of the catalyst dimers **12** (Figure 7).[1-3,21] The reaction of enantiomerically pure (2*S*)- or (2*R*)-DAIB and a dialkylzinc produces stereoselectivity (2*S*,2′*S*)- and (2*R*,2′*R*)-**12**, respectively, while racemic DAIB reacts with the dialkylzinc forms (2*S*,2′*R*)-**12** exclusively. The latter heterochiral dimer having a central unit anti-5/4/5 tricyclic system is more stable than the homochiral compounds with a syn-5/4/5 geometry, as proved by NMR analysis as well as cryoscopic and vapor pressure osmometric molecular weight measurements.[22] This thermodynamic difference coupled with the reaction conditions results in the enormous chirality amplification. The above MO calculations have convinced us of the origin of the thermodynamic preference in the enantiomer recognition of the asymmetric catalysts.

The catalyst **1** is stabilized by dimerization. The calculated dimeric structures **2** are in line with the characteristics of the

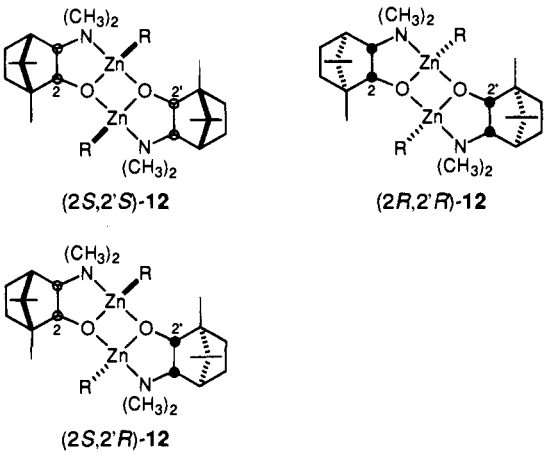

Figure 7. Catalyst dimers in the DAIB-promoted alkylation of aldehydes.

crystallographic geometries of the homochiral and heterochiral dinuclear compounds formed from dimethylzinc and chiral DAIB.[3b] The bicyclo[2.2.1]heptane skeleton in DAIB does exert influence on the structures of the diastereomeric **12**, but even in the prototype **2** where such factors are removed, the meso stereoisomer, *anti*-**2**, is more stable than the chiral isomer, *syn*-**2**, by 3.1 kcal/mol.

(c) Ligand Acceleration. This is a key issue in the efficiency of the catalytic reaction. Although dialkylzincs do not react with aldehydes in hydrocarbon solvents,[23] an addition of β-dialkylamino alcohols or related compounds increases the rate remarkably (Figure 1). The emergence of the ligand acceleration effect[24] is based on the generation of the type **1** catalyst from a dialkylzinc and amino alcohol. The catalyst assembles an aldehyde and dialkylzinc to form the type **5** complex which undergoes the alkyl migration reaction. The tricoordinate Zn catalyst having a polar Zn−O bond tends to be stabilized by forming inactive dimers, but this process is reversible with the amino group playing an important role. Simple alkanols do not act as promoters of the alkylation, because simple alkylzinc

(20) Soulati, J.; Henold, K. L.; Oliver, J. P. *J. Am. Chem. Soc.* **1971**, *93*, 5694−5698. Henold, K.; Soulati, J.; Oliver, J. P. *J. Am. Chem. Soc.* **1969**, *91*, 3171−3174.

(21) Noyori, R. *Science* **1990**, *248*, 1194−1199.

(22) Kitamura, M.; Suga, S.; Niwa, M.; Noyori, R.; Zhai, Z.-X.; Suga, H. *J. Phys. Chem.* **1994**, *98*, 12776−12781.

(23) Boersma, J. In *Comprehensive Organometallic Chemistry*; Wilkinson, G., Stone, F. G. A., Abel, E. W., Eds.; Pergamon Press: Oxford, 1982; Vol. 2, Chapter 16.

(24) Other notable examples: (a) Jacobsen, E. N.; Markó, I.; Mungall, W. S.; Schröder, G.; Sharpless, K. B. *J. Am. Chem. Soc.* **1988**, *110*, 1968−1970. (b) Corey, E. J.; Bakshi, R. K.; Shibata, S. *J. Am. Chem. Soc.* **1987**, *109*, 5551−5553.

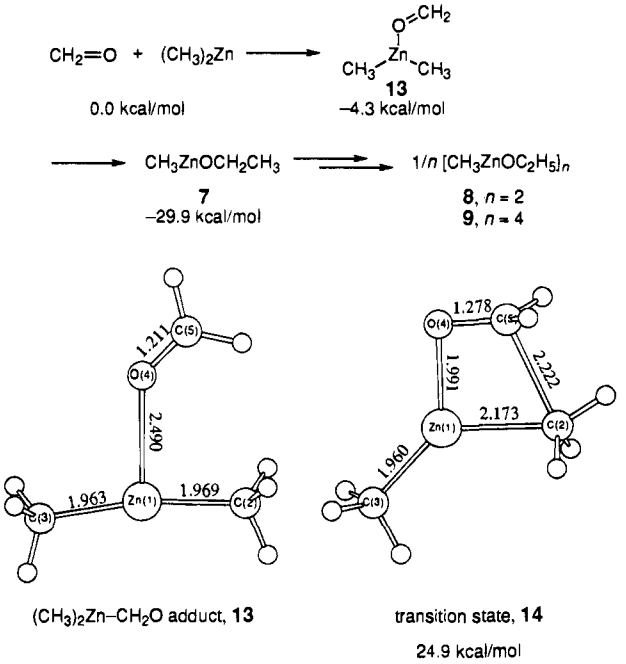

Figure 8. Uncatalyzed reaction between dimethylzinc and formaldehyde. An equimolar mixture of dimethylzinc and formaldehyde is taken as standard for the energy calculation.

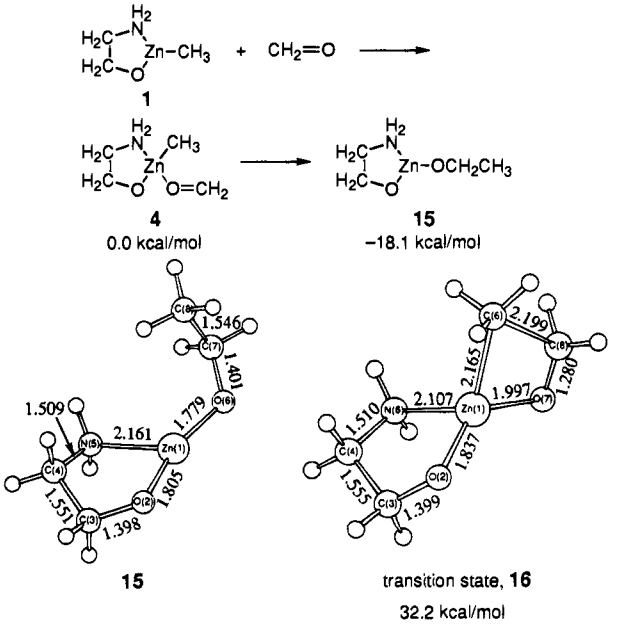

Figure 9. Intramolecular methyl migration in **4**. The complex **4** is taken as standard for the energy calculation.

alkoxides, even with bulky alkoxy groups,[9f] form stable cubic tetramers of type **9**, which do not dissociate into monomeric catalytic species.

In order to infer the reactivity in the absence of amino alcohols, *ab initio* MO calculations were done on the reaction of dimethylzinc and formaldehyde. Figure 8 illustrates the optimized structures of the dimethylzinc−formaldehyde adduct **13** and the transition structure **14**. The reaction of dimethylzinc and formaldehyde gives **13** exothermically by 4.3 kcal/mol, which in turn is transformed to **7** by way of the four-membered transition structure **14**. The methyl migration reaction is calculated to be exothermic by 25.5 kcal/mol but with an activation energy of 29.2 kcal/mol. The latter value is much larger than the 12.4 kcal/mol required for the **5** → **6** conversion in the catalyzed reaction. The difficulty of the uncatalyzed reaction is well understood on both electronic and steric grounds. In order for the reaction to occur, an interaction between the Zn−CH_3 bond and CH_2=O π face is required. This ground-state geometry of the σ complex **13**, however, is not suitable for this process;[15−18] the shape of LUMO developing at C(11) is spatially inappropriate for the acceptance of the Zn-methyl group. The overall reaction of dimethylzinc and formaldehyde is exothermic by 29.9 kcal/mol, and the initial product **7** is further stabilized by the formation of the dimer **8** and tetramer **9**. Thus, the uncatalyzed reaction appears to be thermodynamically allowed but kinetically unfavorable. This organometallic reaction thus needs an amino alcohol as a promoter.

Notably, the quantity of the amino alcohol is very important in obtaining a high yield. The organozinc reaction proceeds smoothly only when a small amount of an amino alcohol is employed; one should not use 100 mol % of the amino alcohol to dialkylzinc. It should be emphasized that the complex **1** is an excellent catalyst for the alkylation but it does not act as alkyl donor. This is due to the lack of reactivity of **4**. Despite the presence of a methyl group and aldehyde on the same Zn atom, **4** is incapable of undergoing intramolecular alkyl transfer. The conversion of **4** to **15** is exothermic by 18.1 kcal/mol but requires activation energy as high as 32.2 kcal/mol (Figure 9). The decrease in the coordination number of the Zn from three to two substantially reduces the exothermicity with respect to the uncatalyzed reaction. The high-energy transition structure **16** is characterized by four-centered geometry, with a short Zn(1)−O(7) distance. Thus, like the uncatalyzed alkylation of Figure 8, this reaction is thermally allowed but kinetically difficult.

Overall, it is concluded that *two Zn atoms per aldehyde are necessary for the alkylation reaction*, consistent with the dependency of the reactivity on the dialkylzinc/amino alcohol stoichiometry. The bifunctional character of the catalyst is inferred from the frontier MOs in Figure 4. The Zn center, as a Lewis acid, activates the aldehyde substrate via interaction with the oxygen nonbonding orbital, while the basic oxygen atom interacts with dialkylzinc. The high electrophilicity of the formaldehyde ligand and eminent nucleophilicity of the methyls attached to the catalyst are inferred from the low LUMO level and high HOMO level (Figure 4).

(d) Prevention of Product Inhibition. In multistep molecular catalysis, all the elementary steps must proceed smoothly. In addition to the reaction-inducing ability of the catalyst as described above, the tetrameric nature of the alkylzinc alkoxide[3b,9] facilitates the catalytic reaction of Figure 1. As is seen in Figure 2 showing the calculated scheme of the model reaction, the initial reaction product **6** is envisaged as an adduct of the alkylzinc alkoxide **7** and catalyst **1**. The cyclic adduct is extremely stable and does not readily dissociate into individual components; this process is highly endothermic (ΔE = +44.4 kcal/mol). The associative reaction of **6** with dimethylzinc or formaldehyde or both, giving **3**, **4**, or **5** together with **7**, is also endothermic by 28.5, 33.0, and 17.9 kcal/mol, respectively. Very high stability in the catalyst−product complex would result in a substantial product inhibition of the catalytic reaction. Fortunately, however, the alkylzinc alkoxide **7** does not exist as a monomer but tends to form stable aggregates to mitigate the endothermicity. The dimerization forming **8** is calculated to occur with an exothermicity of 24.3 kcal/mol of **7**. This value is smaller than 28.5 or 33.0 kcal/mol but larger than 17.9 kcal/mol. Thus, the reaction of the catalyst/product complex **6** with dimethylzinc and formaldehyde giving **5** and **8** becomes 6.5 kcal/mol exothermic. Thus, the formation of the dimeric product **8** is the minimum requirement for establishing the smooth

catalytic cycle of Figure 2. Actually, **7** forms the more stable tetramer **9**. The tetramerization is calculated to take place with an exothermicity of 38.5 kcal/mol of **7**. Then, the bimolecular reaction of **6** and formaldehyde or dimethylzinc, giving **3** or **4** and tetramer **9**, occurs with an exothermicity of 10.0 and 5.5 kcal/mol, respectively. The reaction of **6**, dimethylzinc, and formaldehyde resulting in **5** and **9** is even preferred (ΔE = −20.6 kcal/mol). The high endothermicity of the unimolecular dissociation of **6** into **1** and **7** cannot be subjugated by the high stability of **9**.

The real reaction using a 1:1:1 mixture of the Zn catalyst, benzaldehyde, and dimethylzinc in toluene (Figure 1) indeed forms a stable catalyst/product adduct corresponding to **6**, which is detectable by ^{1}H NMR.[3b] Upon exposure to dimethylzinc or benzaldehyde, it immediately produces the type **9** tetrameric alkoxide. Thus, the catalytic reaction of Figure 1 is themodynamically driven by the formation of the stable tetramer. The tetramer is independent of the catalytic species and does not disturb the catalytic cycle.

Conclusion

Although addition of dimethylzinc to formaldehyde is highly exothermic, the reaction does not occur without an amino alcohol. A key issue for the efficiency of the catalytic reaction is the Lewis acid/Lewis base bifunctional property, as seen in the tricoordinate complex **1** that forms the mixed ligand complex **5**. The Lewis acidic Zn center accommodates formaldehyde via the oxygen nonbonding orbital to increase the electrophilic character at the carbon, whereas the neighboring oxygen atom coordinates to dimethylzinc, enhancing the nucleophilic character of the methyl groups. The frontier MOs in **5** are highly localized on the aldehyde carbon region (LUMO) and the Zn−CH_3 bonds (HOMO). In addition, the LUMO level is 1.25 eV lower than free formaldehyde, and the HOMO is 1.31 eV higher than dimethylzinc. Such effects are also reflected in the geometry. In going from free formaldehyde to **5**, the C=O bond is 0.7% elongated, whereas, the dative interaction between the oxygen atom and dimethylzinc generates a bent dimethylzinc structure in which the Zn−CH_3 distances are 2−3% longer than in the free, linear structure. The intramolecular methyl migration occurs from **5** via 4/4 bicyclic transition states **10** to form the catalyst−alkoxide product adduct **6**. Product inhibition can be avoided when a stable tetrameric methylzinc ethoxide, **9**, is formed by reacting **6** with formaldehyde or more readily with dimethylzinc. The tricoordinate Zn catalyst **1** is stabilized by dimerization, where the achiral anti dimer **2** is more stable than the chiral syn dimer **2**, consistent with the experimentally observed chirality amplification phenomenon. The dimerization process is reversible, with the amine moiety is playing an important role.

Supplementary Material Available: Tables giving calculated bond lengths and angles for **1**−**16** and related compounds (47 pages). This material is contained in many libraries on microfiche, immediately follows this article in the microfilm version of the journal, can be ordered from the ACS, and can be downloaded from the Internet; see any current masthead page for ordering information and Internet access instructions.

JA950579E